ACADEMIC PRESS

NONVIRAL VECTORS *for* GENE THERAPY

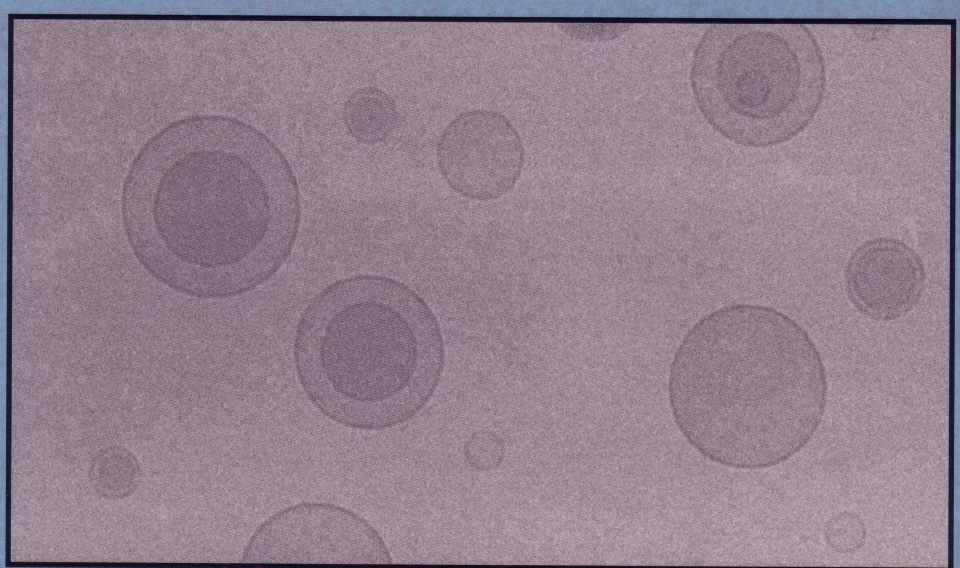

Edited by

Leaf Huang

Mien-Chie Hung

Ernst Wagner

CHAPTER 5

Self-Assembled Structures of Lipid/DNA Nonviral Gene Delivery Systems from Synchrotron X-Ray Diffraction

Cyrus R. Safinya and Ilya Koltover
Materials Department, Physics Department, and Biochemistry and Molecular Biology Program, University of California, Santa Barbara, California

There is now a surge of activity in developing synthetic nonviral gene delivery systems for gene therapeutic applications because of their low toxicity, nonimmunogenicity, and ease of production. Cationic liposome/DNA (CL/DNA) complexes have shown gene expression *in vivo* in targeted organs, and human clinical protocols are ongoing. Moreover, the single largest advantage of nonviral over viral methods for gene delivery is the potential of transferring extremely large pieces

of DNA into cells. This was clearly demonstrated when partial fractions of order 1 Mega base pairs of human artificial chromosome were recently transferred into cells using cationic liposomes as a vector, although extremely inefficiently. However, because the mechanism of action of CL/DNA complexes remains largely unknown, transfection efficiencies are at present very low and vary by up to a factor of 100 in different cell lines. The low transfection efficiencies with nonviral delivery methods are the result of poorly understood transfection-related mechanisms at the molecular and self-assembled levels.

In this chapter we review recent work aimed at elucidating the precise self-assembled structures of CL/DNA complexes by the quantitative techniques of synchrotron X-ray diffraction. Recently, we found that when DNA is mixed with cationic liposomes composed of DOPC/DOTAP, the result is a topological transition into condensed CL/DNA complexes with a multilamellar structure (L_α^C) composed of DNA monolayers sandwiched between cationic lipid bilayers. The existence of a completely different columnar inverted hexagonal H_{II}^C liquid-crystalline state in CL/DNA complexes was also demonstrated using synchrotron small-angle X-ray diffraction. The commonly used neutral helper lipid DOPE is found to induce the L_α^C to H_{II}^C structural transition by controlling the spontaneous curvature $C_o = 1/R_o$ of the lipid monolayer. Further, an entirely new class of helper molecules was introduced that controls the membrane bending rigidity κ and gives rise to a distinctly different pathway to the H_{II}^C phase. Significantly, optical microscopy has revealed that in contrast to the weakly transfectant L_α^C complexes that bind stably to anionic vesicles (models of cellular membranes), the more transfectant H_{II}^C complexes are unstable, rapidly fusing and releasing DNA upon adhering to anionic vesicles. The observations underscore the importance of self-assembled structure to "early-stage" gene delivery events and provide direct imaging support for either a mechanism of DNA escape from anionic endosomal vesicles or fusion of CL/DNA complexes with cell plasma membrane.

I. INTRODUCTION

Gene therapy depends on the successful transfer and expression of extracellular DNA to mammalian cells, with the aim of replacing a defective gene or adding a missing one (Friedmann, 1997; Felgner, 1997; Miller, 1998; Crystal, 1995; Zhu *et al.*, 1993; Nabel *et al.*, 1993; Mulligan, 1993; Felgner and Rhodes, 1991; Behr, 1994; Remy *et al.*, 1994; Singhal and Huang, 1994; Lasic and Templeton, 1996; Marhsall, 1995). At present, viral-based vectors (retroviruses, adenoviruses, adeno-associated viruses) are the most common gene carriers used by researchers developing gene delivery systems because of their high efficiency of transfer and expression (Friedmann, 1997; Crystal, 1995; Mulligan, 1993). Each vector has advantages and disadvantages and it will be many years before the optimal vector is

designed. Retrovirus vectors integrate into the host chromosomes, providing the prospect of lifelong cure. However, their disadvantages include the possibility that the crippled virus may potentially become infectious through recombination, the fact that the currently used vectors only integrate in dividing host cells, the limited size of the therapeutic gene that may be packed into the crippled viral gene, and the technical difficulty associated with production of high titer virus stocks (Friedmann, 1997; Crystal, 1995). Because adenovirus-based vectors do not integrate their genes into the chromosome but instead act transiently, repeated applications are necessary, which has resulted in undesirable immune responses in recent clinical trials. Adeno-associated viruses integrate into the host chromosomes but have a very small capsid size and are therefore limited in the size of the therapeutic gene that they may carry. Current viral vectors have a maximum gene-carrying capacity of 40k base pairs (Friedmann, 1997; Crystal, 1995).

At the same time there has been much recent activity for the development of synthetic nonviral gene delivery systems (Friedmann, 1997; Felgner, 1997; Miller, 1998; Zhu *et al.,* 1993; Nabel *et al.,* 1993; Felgner and Rhodes, 1991; Behr, 1994; Remy *et al.,* 1994; Singhal and Huang, 1994; Lasic and Templeton, 1996). The conventional nonviral transfer methodologies, which have transfection rates significantly lower than viral transfection rates, include anionic liposomes that encapsulate nucleic acid, calcium phosphate precipitation, and use of polycationic reagents (DEAE-dextran or polylysine). Some of the advantages of using nonviral vectors for gene delivery include the fact that plasmid DNA constructs used in deliveries are more readily prepared than viral constructs, they have no viral genes to cause disease, and that synthetic carriers are nonimmunogenic due to a lack of proteins.

The entire field of gene therapy based on synthetic nonviral delivery systems has recently undergone a renaissance since the initial paper by Felgner *et al.* (1987), which was soon to be followed by numerous other groups demonstrating gene expression *in vivo* in targeted organs (Zhu *et al.,* 1993; Singhal and Huang, 1994), and in human clinical trials (Nabel *et al.,* 1993). Felgner *et al.* discovered that cationic liposomes (CLs) (closed bilayer membrane shells of lipid molecules; see Fig. 1) when mixed with DNA to form (CL/DNA) complexes with an overall positive charge, enhance transfection (i.e., the transfer of plasmid into cells followed by expression).

They hypothesized that this was because CL/DNA complexes adsorbed more effectively to the anionic plasma membrane of mammalian cells via the electrostatic interactions. Compared to other nonviral delivery systems, cationic liposomes tend to mediate a higher level of transfection in the majority of cell lines studied to date (Lasic and Templeton, 1996). Using cationic liposomes, gene expression of chloramphenicol acetyltransferase (CAT) activity has been found in mice lungs and brain (Brigham *et al.,* 1989; Hazinski *et al.,* 1991; Ono *et al.,* 1990), and in brain tissue of frog embryos (Malone, 1989; Holt *et al.,* 1990). *In vivo* CAT expression of aerosol-administered plasmid DNA (pCIS-CAT) complexed with cationic liposomes in mouse lung has also been demonstrated (Stribling *et al.,* 1992).

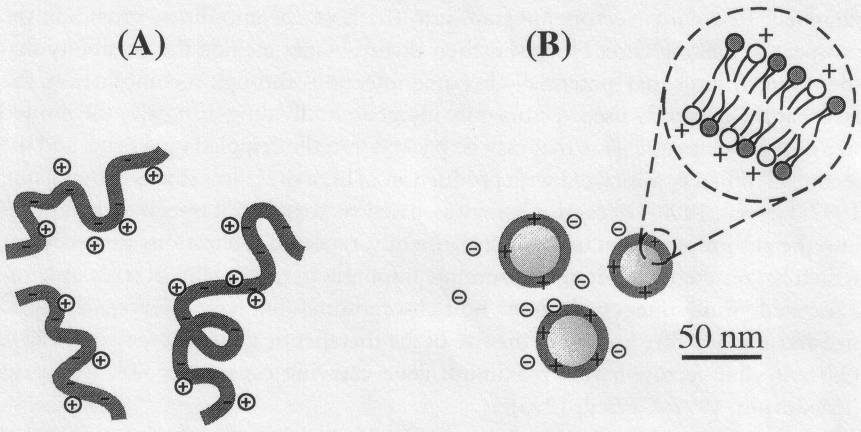

Figure 1 (A) Schematic of anionic DNA polyelectrolytes with cationic counterions condensed on the backbone due to Manning condensation. (B) Schematic of cationic liposomes (or vesicles), which consist of spherical membranes containing a bilayer of lipid molecules normally consisting of a mixture of cationic and neutral lipids. (Bar for (B) only.)

Without doubt, one of the principal and most exciting advantages of nonviral over viral methods for gene delivery is the potential of transferring and expressing (transfecting) large pieces of DNA into cells. The proof of this concept was clearly demonstrated when partial sections of first-generation human artificial chromosomes (HACs) of order 1 Mbp were transferred into cells with CLs, although extremely inefficiently (Harrington *et al.*, 1997; Roush, 1997). The future development of HAC vectors will be extremely important for gene therapy applications; because of their very large size capacity HACs would have the ability of delivering not only entire human genes (in many cases exceeding 100k bp) but also their regulatory sequences, which are needed for the spatial and temporal regulation of gene expression.

While the transfection rates and reproducibility in many cells have been found to be enhanced using CL/DNA complexes compared to other more traditional nonviral delivery systems, the mechanism of transfection via cationic liposomes remains largely unknown (Friedmann, 1997; Felgner, 1997; Miller, 1998; Crystal, 1995; Zhu *et al.*, 1993; Nabel *et al.*, 1993; Mulligan, 1993; Felgner and Rhodes, 1991; Behr, 1994; Remy *et al.*, 1994; Singhal and Huang, 1994; Lasic and Templeton, 1996; Marhsall, 1995). At present hundreds of plasmid DNA molecules are required for successful gene transfer and expression. The low transfection efficiencies with nonviral methods results from a general lack of knowledge regarding (1) the structures of CL/DNA complexes and (2) their interactions with cell membranes and events leading to release of DNA in the cytoplasm for delivery within the nucleus. We are now beginning to understand the precise nature of the self-

assembled structures of CL/DNA complexes in different lipid-membrane systems (Raedler *et al.*, 1997; Spector and Schnur, 1997; Seachrist, 1997; Salditt *et al.*, 1997; Safinya *et al.*, 1998; Raedler *et al.*, 1998; Salditt *et al.*, 1998; Lasic *et al.*, 1997; Pitard *et al.*, 1997; Koltover *et al.*, 1998). The transfection efficiencies of nonviral delivery methods may be improved through insights into transfection-related mechanisms at the molecular and self-assembled levels.

Aside from the medical and biotechnological ramifications in gene therapy and gene and drug therapeutics, research on CL/DNA complexes should also shed light on other problems in biology. The development of efficient HAC vectors in the future, which will most likely occur once efficient synthetic nonviral delivery systems have been developed, is a long-range goal in studies designed to characterize chromosome structure and function. Furthermore, molecular biology studies would benefit substantially from the ability of transfecting hard-to-transfect cell lines with synthetic delivery systems; for example, in studies designed to characterize the structure of promoters of human genes in the appropriate cell lines.

DNA chains dissolved in solution are known to give rise to a rich variety of condensed and liquid crystalline phases. Studies show regular DNA condensed morphologies induced by multivalent cations (Bloomfield, 1991) and liquid crystalline (LC) phases at high concentrations of DNA both *in vitro* (Livolant and Leforestier, 1996) and *in vivo* in bacteria (Reich *et al.*, 1994). More recently there has been a flurry of experimental and theoretical work on DNA chains mixed with cationic liposomes. Early on oligo-lamellar structures had been reported in cryo-TEM studies by Gustafsson *et al.* (1995). Freeze–fracture electron microscopy study by Sternberg *et al.* had also observed isolated DNA chains coated with a lipid bilayer (Sternberg *et al.*, 1994). One of the self-assembled structures that forms spontaneously when DNA (a negative polyelectrolyte) is complexed with cationic liposomes containing a specific type of lipid is a multilayer assembly of DNA sandwiched between bilayer membranes shown schematically in Fig. 2 (Raedler *et al.*, 1997; Spector and Schnur, 1997; Seachrist, 1997; Salditt *et al.*, 1997; Safinya *et al.*, 1998; Raedler *et al.*, 1998; Salditt *et al.*, 1998; Lasic *et al.*, 1997; Pitard *et al.*, 1997).

The structure and thermodynamic stability of these CL/DNA complexes has also been the subject of much recent theoretical work (May and Ben-Shaul, 1997; Dan, 1998; Bruinsma, 1998; Bruinsma and Mashl, 1998; Harries *et al.*, 1998; O'Hern and Lubensky, 1998; Golubovic and Golubovic, 1998). Analytical and numerical studies of DNA–DNA interactions bound between membranes show the existence of a novel long-range repulsive electrostatic interaction (Bruinsma, 1998, Bruinsma and Mashl, 1998; Harries *et al.*, 1998). Theoretical work on CL/DNA complexes has also led to the realization of a variety of novel new phases of matter in DNA/lipid complexes (O'Hern and Lubensky, 1998; Golubovic and Golubovic, 1998). In particular, a novel new "sliding columnar phase," which remains to be discovered experimentally, is predicted where the positional coherence between DNA molecules in adjacent layers is lost without destroying orientational

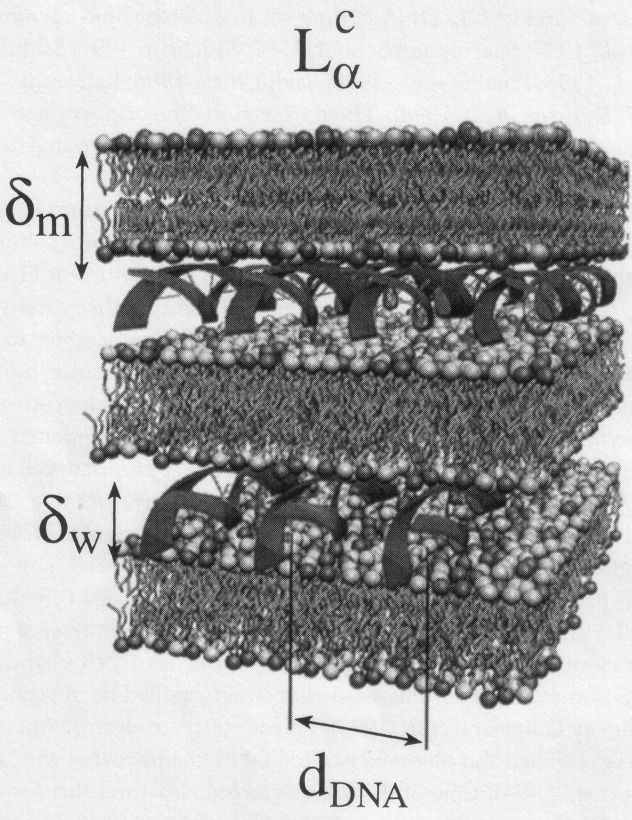

Figure 2 Schematic of the lamellar $L_\alpha{}^C$ phase of cationic liposome/DNA (CL/DNA) complexes with alternating lipid bilayer and DNA monolayer. The DNA interaxial spacing is d_{DNA}. The interlayer spacing is $d = \delta_w + \delta_m$. [Redrawn from Raedler *et al.*, (1997).]

coherence of the chains from layer to layer. This new phase would be a remarkable new phase of matter if it exists, and shares many fascinating similarities with flux lattices in superconductors.

In its own right from a biophysics perspective, it is important to explore the phase behavior of DNA attached to membranes in two dimensions (Fig. 2) as a tractable experimental and theoretical system for understanding DNA condensation. The mechanisms of DNA condensation *in vivo* (i.e., packing in a small space) are poorly understood (Lewin, 1997). DNA condensation and decondensation that happens, for example, during the cell cycle in eukaryotic cells involves different types of oppositely charged polyamines, peptides, and proteins (e.g., histones)

where the nonspecific electrostatic interactions are clearly important. In bacteria that are the simplest cell types, it is thought that multivalent cationic polyamine molecules (spermine, spermidine) are responsible for DNA condensation in the three-dimensional space of the cell cytoplasm. DNA-membrane interactions might also provide clues for the relevant molecular forces in the packing of DNA in chromosomes and viral capsids.

II. SYNCHROTRON X-RAY DIFFRACTION STUDIES

A. The Lamellar L_α^C Phase of CL/DNA Complexes

We have recently carried out a combined *in situ* optical microscopy and synchrotron X-ray diffraction (XRD) study of CL/DNA complexes Raedler *et al.*,, 1997; Spector and Schnur, 1997; Seachrist, 1997; Salditt *et al.*, 1979; Safinya *et al.*, 1998; Raedler *et al.*, 1998; Salditt *et al.*, 1998) where the cationic liposomes consisted of mixtures of neutral (so called "helper lipid") DOPC (dioleoyl phosphatidyl cholin) and cationic DOTAP (dioleoyl trimethylammonium propane) (Fig. 3). High-resolution small-angle X-ray diffraction has revealed that the structure is different from the hypothesized "bead-on-string" structure, originally proposed by Felgner *et al.* for CL/DNA complexes in their seminal paper (Felgner and Rhodes, 1991; Felgner *et al.*, 1987), which pictures the DNA strand decorated with distinctly attached cationic liposomes. The addition of linear λ-phage DNA (48,502 bp, contour length = 16.5 μm) to binary mixtures of cationic liposomes (mean diameter of 70 nm) induces a topological transition from liposomes into collapsed condensates in the form of optically birefringent liquid crystalline (LC) globules with size on the order of 1 μm.

We show in Fig. 4(A) differential–interference–contrast (DIC) optical images of CL/DNA complexes for four lipid (L) to λ-DNA (D) ratios (L = DOTAP + DOPC (1/1)) (see Endnote 1). Similar images are observed with λ-DNA replaced by the pBR322 plasmid (4361 bp) DNA or DOPC replaced by DOPE. At low DNA concentrations (Fig. 4A, $L/D = 50$), in contrast to the pure liposome solution where no objects greater than 0.2 μm are seen, 1-μm large globules are observed. The globules coexist with excess liposomes. As more DNA is added, the globular condensates form larger chain-like structures (Fig. 4A, $L/D = 10$). At $L/D \approx 5$ the chain-like structures flocculate into large aggregates of distinct globules. For $L/D < 5$, the complex size was smaller and stable in time again (Fig. 4A, $L/D = 2$), and coexisted with excess DNA. Fluorescent microscopy of the DNA (labeled with YoYo) and the lipid (labeled with Texas Red-DHPE) also showed that the individual globules contain both lipid and DNA (see Fig. 15A and B). Polarized microscopy also shows that the distinct globules are birefringent indicative of their liquid crystalline nature.

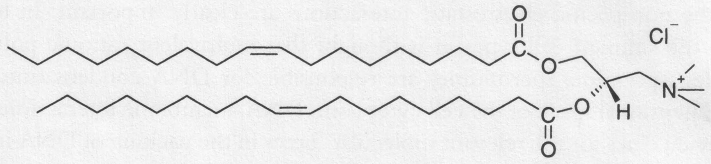

DOTAP (cationic lipid)

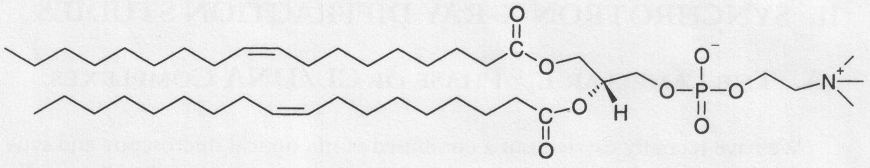

DOPC (neutral, helper lipid)

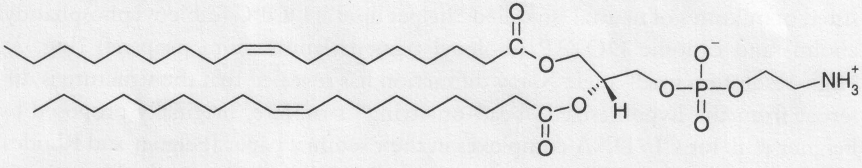

DOPE (neutral, helper lipid)

Figure 3 Top: The cationic lipid DOTAP (dioleoyl trimethylammonium propane). Middle: The neutral helper lipid DOPC (dioleoylphosphatidylcholine). Bottom: The neutral helper lipid DOPE (dioleoylphosphadtidylethanolamine). The neutral lipid is referred to as the "helper lipid."

The size dependence of the complexes as a function of L/D (Fig. 4B) was independently measured by dynamic light scattering (Microtrac UPA 150, Leeds and Northrup). The large error bars represent the broad polydispersity of the system. The size dependence of the aggregates can be understood in terms of a charge-stabilized colloidal suspension. The charge of the complexes was measured by their electrophoretic mobility in an external electric field. For $L/D > 5$ (Fig. 4A; $L/D = 50$ or 10) the complexes are positively charged, while for $L/D < 5$ (Fig. 4A; $L/D = 2$) the complexes are negatively charged. The charge reversal is in good agreement with the stoichiometrically expected charge balance of the components DOTAP and DNA at $L/D = 4.4$ (Wt./Wt.), where L = DOTAP + DOPC in equal weights. Thus, the positively and negatively charged globules at $L/D = 50$ and $L/D = 2$, respectively, repel each other and remain separate, while as L/D approaches 5, the nearly neutral complexes collide and tend to stick due to van der Waals attraction.

The high resolution synchrotron small-angle X-ray scattering (SAXS) experi-

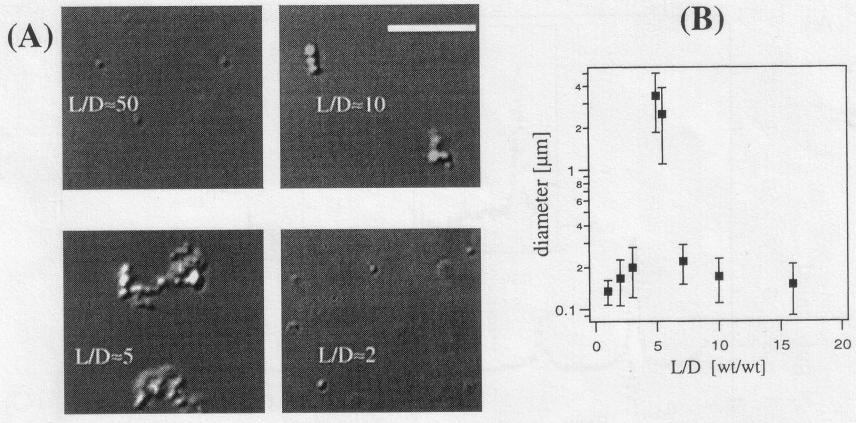

Figure 4 (A) High-resolution DIC optical images of CL/DNA complexes forming distinct condensed globules in mixtures of different lipid-to-DNA weight ratio (L/D). $L/D = 4.4$ is the isoelectric point, CL/DNA complexes are positively charged for $L/D = 50$ and 10, and negatively charged for $L/D = 2$. The positive (negative) regime contains excess lipid (DNA). (B) Average size of the lipid/DNA complexes measured by dynamic light scattering. Bar is 10 μm. [Adapted from Raedler *et al.*, (1997).]

ments carried out at the Stanford Synchrotron Radiation Laboratory revealed unexpected structures for mixtures of CLs and DNA (Raedler *et al.*, 1997; Salditt *et al.*, 1997; Seachrist, 1997; Spector and Schnur, 1997). SAXS data of dilute (Φ_w = the volume fraction of water = 98.6% ± 0.3%) DOPC/DOTAP (1/1)–λ-DNA mixtures as a function of L/D (L = DOPC + DOTAP) (Fig. 5A) are consistent with a complete topological rearrangement of liposomes and DNA into a multilayer structure with DNA intercalated between the bilayers (Fig. 2, denoted L_α^c). Two sharp peaks at $q = 0.0965 \pm 0.003$ and 0.193 ± 0.006 Å^{-1} correspond to the (00L) peaks of a layered structure with an interlayer spacing d ($= \delta_m + \delta_w$), which is in the range 65.1 ± 2 Å (Fig. 5B, open squares). The membrane thickness and water gap are denoted by δ_m and δ_w, respectively (Fig. 2). The middle broad peak q_{DNA} arises from DNA-DNA correlations and gives $d_{DNA} = 2\pi/q_{DNA}$ (Fig. 5B, solid circles). The multilamellar L_α^c structure with intercalated DNA is also observed in CL/DNA complexes containing supercoiled DNA both in water and also in Dulbecco's Modified Eagle's Medium used in transfection experiments (Lin *et al.*, in preparation). This novel multilamellar structure of the CL/DNA complexes is observed to protect DNA from being cut by restriction enzymes (Raedler *et al.*, 1998).

In the absence of DNA, membranes composed of mixtures of DOPC and the cationic lipid DOTAP (1/1) exhibit strong long-range interlayer electrostatic repulsions that overwhelm the van der Waals attraction (Roux and Safinya, 1988; Safinya 1989). In this case, as the volume fraction Φ_w of water is increased, the L_α phase swells and d is given by the simple geometric relation $d = \delta_m/(1 - \Phi_w)$. The

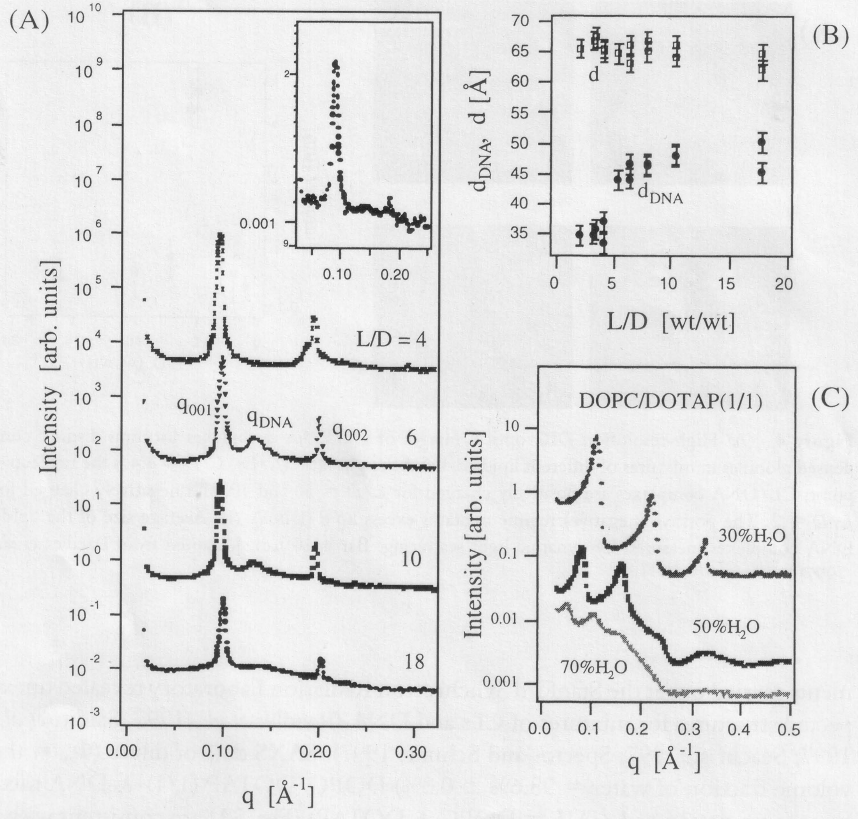

Figure 5 (A) A series of high-resolution synchrotron SAXS scans of CL/DNA complexes in excess water as a function of different lipid-to-DNA weight ratio (L/D). The Bragg-reflections at $q_{001} = 0.096$ Å^{-1} and $q_{002} = 0.192$ Å^{-1} result from the multilamellar $L_\alpha{}^c$ structure with intercalated monolayer DNA (see Fig. 2). The intermediate peak at q_{DNA} is due to the DNA-interaxial spacing d_{DNA} (Fig. 2). *Inset*: SAXS scan of an extremely dilute (lipid + DNA = 0.014% volume in water) λ-DNA-DOPC/DOTAP (1/1) complex at $L/D = 10$, which shows the same features as the more concentrated mixtures and confirms the multilamellar structure (with alternating lipid bilayer and DNA monolayers) of very dilute mixtures typically used in clinical gene therapy applications. (B) The spacings d and d_{DNA} as a function of L/D show that (i) d is nearly constant and (ii) there are two distinct regimes of DNA packing, one where the complexes are positive ($L/D > 5$, d_{DNA} 46 Å), and the other regime where the complexes are negative ($L/D < 5$, d_{DNA} 35 Å). (C) SAXS scans of the lamellar L_α phase of DOPC/DOTAP (cationic)-water mixtures done at lower X-ray resolution on a rotating anode X-ray generator. A dilution series of 30% ($d = 57.61$ Å), 50% (d = 79.49 Å), and 70% ($d = 123.13$ Å) H_2O by weight is shown. [Adapted from Raedler *et al.*, (1997).]

SAXS scans in Fig. 5(C) show this behavior with the (00L) peaks moving to lower q as Φ_w increases. From d ($= 2\pi/q_{00L}$) at a given Φ_w we obtain $\delta_m = 39 \pm 0.5$ Å for DOPC/DOTAP (1/1). Liposomes made of DOPC/DOTAP(1/1) with $\Phi_w \approx 98.5\%$ do not exhibit Bragg diffraction in the small wave-vector range covered in Fig. 5(A).

The DNA that condenses on the CLs strongly screens the electrostatic interaction between lipid bilayers and leads to condensed multilayers. The average thickness of the water gap $\delta_w = d - \delta_m = 65.1$ Å $- 39$ Å $= 26.1$ Å ± 2.5 Å is just sufficient to accommodate one monolayer of B-DNA (diameter ≈ 20 Å) including a hydration shell (Podgornik *et al.*, 1994). We see in Fig. 5(B) that d is almost constant as expected, for a monolayer DNA intercalate (Fig. 2). In contrast, as L/D decreases from 18 to 2, d_{DNA} suddenly decreased from ≈ 44 Å in the positively charged regime just above $L/D = 5$ (near the stoichiometric charge neutral point $L/D = 4.4$) to ≈ 37 Å for the negatively charged regime (Fig. 5B). In these distinctly different packing regimes, L_α^c complexes coexist with excess giant liposomes in the positive regime and with excess DNA in the negative regime. The excess DNA may in fact have a lipid bilayer coating as earlier freeze–fracture studies by Sternberg *et al.* had found ((Sternberg *et al.*, 1994).

The DNA/lipid condensation can be understood to occur as a result of release of "bound" counterions in solution. DNA in solution (Fig. 6A) has a bare length between negative charges (phosphate groups) equal to $b_o = 1.7$ Å. This is substantially less than the Bjerrum length in water, $b_j = 7.1$ Å, which corresponds to the distance where the Coulomb energy between two unit charges is equal to the thermal energy $k_B T$. A nonlinear Poisson–Boltzmann analysis shows that counterions will condense on the DNA backbone until the Manning parameter $\xi = b_j/b'$ approaches 1 (Manning, 1969). (b' is the renormalized distance between negative charges after counterion condensation.) A similar analysis shows that counterions also condense near the surface of two-dimensional membranes (i.e., within the Gouy–Chapman layer) (Zimm and Le Bret, 1983). Through DNA/lipid condensation the cationic lipid tends to fully neutralize the phosphate groups on the

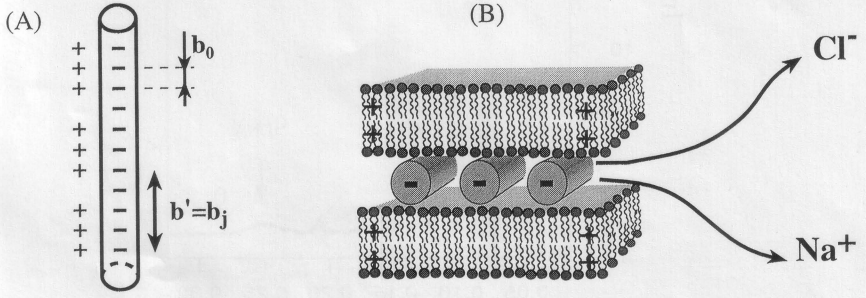

Figure 6 (A) Schematic of double-stranded DNA molecule with a bare distance between negative charges of $b_o = 1.7$ Å. From nonlinear Poisson–Boltzmann we know that positive counterions condense on DNA until the renormalized distance between the negative charges b' equals the Bjerrum length, which is $b_j = 7.1$ Å in water. (B) Schematic drawing showing that as DNA condenses onto the cationic membrane there is a simultaneous release of counterions and a gain in the entropy of solution when the previously condensed counterions (Na^+ on DNA and Cl^- near the cationic liposome membrane) leave the immediate vicinity of DNA and the cationic membrane respectively.

DNA, in effect replacing and releasing the originally condensed counterions in solution. Thus, the driving force for higher order self-assembly is the release of counterions, which were one-dimensionally bound to DNA and two-dimensionally bound to cationic membranes, into solution (Fig. 6B).

The precise nature of the packing structure of λ-DNA within the lipid layers can be elucidated by conducting a lipid dilution experiment in the isoelectric point regime of the complex. In these experiments the total lipid (L = DOTAP + DOPC) is increased while the charge of the overall complex, given by the ratio of cationic DOTAP to DNA, is kept constant at DOTAP/DNA = 2.20. The SAXS scans in Fig. 7 (arrow points to the DNA peak) show that $d_{DNA} = 2\pi/q_{DNA}$ increases

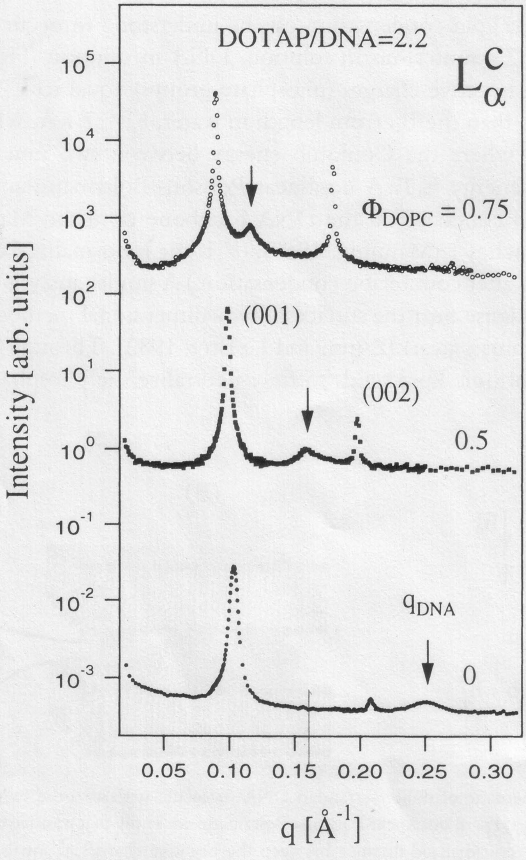

Figure 7 SAXS scans of CL/DNA complexes at constant DOTAP/DNA = 2.2 (at the isoelectric point) with increasing DOPC/DOTAP, which shows the DNA peak (arrow) moving toward smaller q as L/D (and Φ_{DOPC}) increases. L = DOTAP + DOPC, D = DNA. [Adapted from Raedler *et al.*, (1997); Salditt *et al.*, (1997).]

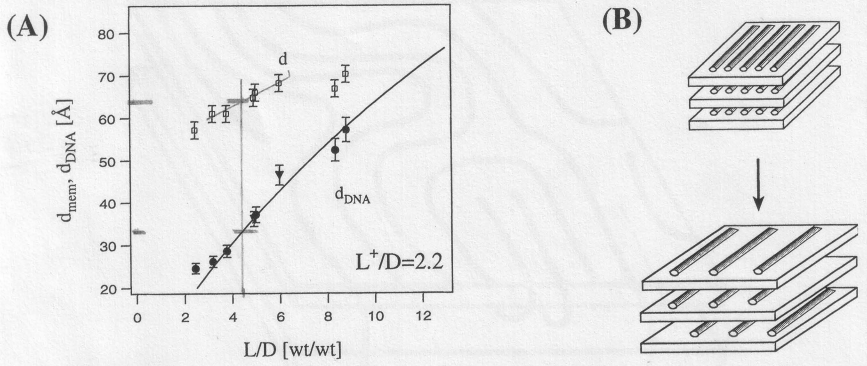

Figure 8 (A) The DNA interaxial distance d_{DNA} and the interlayer distance d in the L_α^c phase (Fig. 2) plotted as a function of lipid/DNA (L/D) (wt/wt) ratio at the isoelectric point of the complex DOTAP/DNA = 2.2. d_{DNA} is seen to expand from 24.5 Å to 57.1 Å. The solid line through the data is the prediction of a packing calculation where the DNA chains form a space-filling one-dimensional lattice. (B) Schematic drawing of DNA/membrane multilayers showing the increase in distance between DNA chains as the membrane charge density is decreased (i.e., as Φ_{DOPC} increases) at the isoelectric point.

with lipid dilution from 24.54 Å to 57.1 Å as Φ_{DOPC}, the weight fraction of DOPC in the DOPC/DOTAP cationic liposome mixtures, increases from 0 to 0.75 (or equivalently increasing L/D between 2.2 and 8.8). The most compressed interaxial spacing of 24.55 Å at $\Phi_{DOPC} = 0$ approaches the short-range repulsive hard-core interaction of the B-DNA rods containing a hydration layer (Pogornik *et al.*, 1994). Figure 8(A) plots d and d_{DNA} as a function L/D.

The observed behavior is depicted schematically in Fig. 8(B) showing that as we add neutral lipid (at the isoelectric point) and therefore expand the total cationic surface we expect the DNA chains to also expand and increase their interaxial spacing. The solid line in Fig. 8(A) is derived from the simple geometric packing relationship $d_{DNA} = (A_D/\delta_m)\,(\rho_D/\rho_L)\,(L/D)$, which equates the cationic charge density (due to the mixture $DOTAP^+$ and DOPC) with the anionic charge density (due to DNA^-). Here, $\rho_D = 1.7$ (g/cc) and $\rho_L = 1.07$ (g/cc) denote the densities of DNA and lipid respectively, δ_m the membrane thickness, and A_D the DNA area. $A_D = Wt(\lambda)/(\rho_D L(\lambda)) = 186$ Å^2, $Wt(\lambda)$ = weight of λ-DNA = 31.5 * 10^6/(6.022 * 10^{23}) g, and $L(\lambda)$ = contour length of λ -DNA = 48502 * 3.4 Å.

The agreement between the packing relationship (solid line) with the data over the measured interaxial distance from 24.5 Å to 57.1 Å (Fig. 8A) is quite remarkable given the fact that there are no adjustable parameters. The variation in the interlayer spacing d ($= \delta_w + \delta_m$) (Fig. 8A, open squares) arises from the increase in the membrane bilayer thickness δ_m as L/D increases (each DOPC molecule is about 4 Å to 6 Å longer than a DOTAP molecule). The observation, of a *variation in the DNA interaxial distance* as a function of the lipid to DNA (L/D) ratio in multilayers (Fig. 8A), unambiguously demonstrates that x-ray diffraction directly probes the

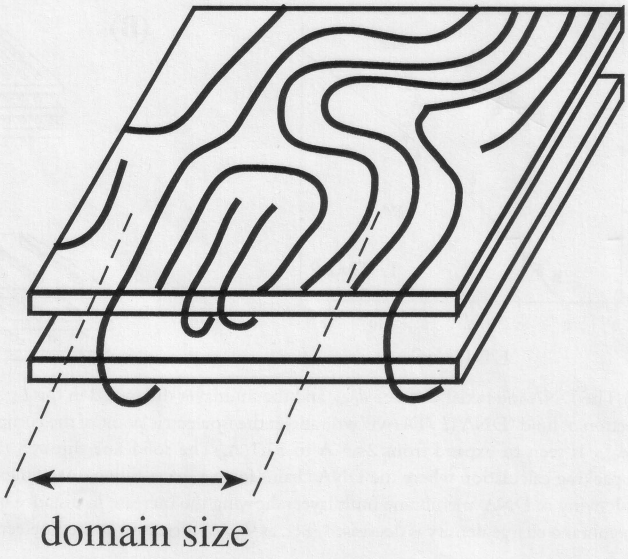

Figure 9 A schematic drawing of the local arrangement of DNA in the interior of the L_{α}^{c} cationic lipid DNA complex consistent with the X-ray diffraction data taking into account the broad width of the DNA peak due to the finite coherent domain size of the DNA chains adsorbed on lipid bilayers. The average domain size of the one-dimensional lattice of DNA chains derived from the width of the DNA peaks is about 10 unit cells.

DNA behavior in multilayer assemblies. From the linewidths of the DNA peaks (Fig. 7) the 1D lattice of DNA chains is found to consist of domains extending to near 10 neighboring chains (Salditt *et al.*, 1997, 1998). Thus, the CL/DNA complex is self-assembled into a new "hybrid" phase of matter, namely, a coupled two-dimensional smectic phase of DNA chains coupled to lipid bilayers of a three-dimensional smectic phase (Fig. 9). On larger length scales the lattice would melt into a 2D nematic phase of chains due to dislocations (O'Hern and Lubensky, 1998; Golubovic and Golubovic, 1998).

B. The Inverted Hexagonal H_{II}^{C} Phase of CL/DNA Complexes

A commonly used helper lipid in CL/DNA mixtures is DOPE (dioleoylphosphatidylethanolamine), shown in Fig. 3. Further, it is empirically known that transfection efficiency in mammalian cells is typically improved in CL/DNA complexes that contain DOPE instead of DOPC as the helper lipid (Felgner *et al.*, 1994; Farhood *et al.*, 1995; Hui *et al.*, 1996). Recent X-ray diffraction shows that DOPE-

containing complexes may give rise to a completely different columnar inverted hexagonal H_{II}^{C} liquid-crystalline structure (Fig. 11).

We show in Fig. 10 SAXS scans in positively charged CL/DNA complexes

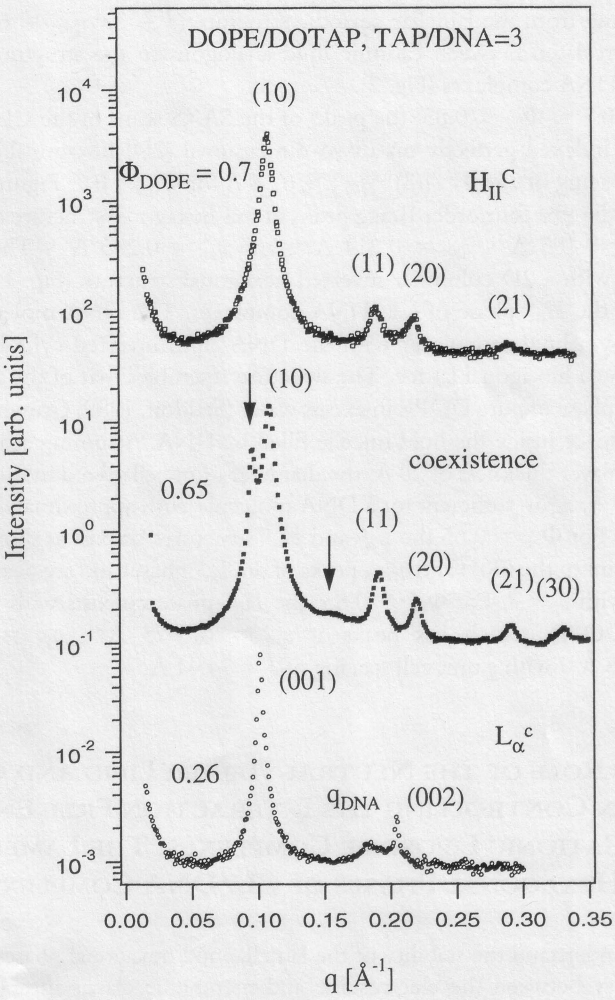

Figure 10 Synchrotron SAXS patterns of the lamellar L_{α}^{C} and columnar inverted hexagonal H_{II}^{C} phases of positively charged CL/DNA complexes as a function of increasing weight fraction Φ_{DOPE}. At $\Phi_{DOPE} = 0.26$, the SAXS results from a single phase with the lamellar L_{α}^{C} structure shown in Fig. 2. At $\Phi_{PE} = 0.7$, the SAXS scan results from a single phase with the columnar inverted hexagonal H_{II}^{C} structure shown in Fig. 11. At $\Phi_{DOPE} = 0.65$, the SAXS shows coexistence of the L_{α}^{C} (arrows) and H_{II}^{C} phases. [Adapted from Koltover *et al.*, (1998).]

for DOTAP/DNA (wt./wt.) = 3 as a function of increasing Φ_{DOPE} (weight fraction of DOPE) in the DOPE/DOTAP cationic liposome mixtures (Koltover *et al.*, 1998). We find that the internal structure of the complex changes completely with increasing DOPE/DOTAP ratios. SAXS data of complexes with $\Phi_{PE} = = 0.26$ and 0.70 clearly show the presence of two different structures. At $\Phi_{PE} = 0.26$, SAXS of the lamellar $L_\alpha{}^C$ complex shows sharp peaks at $q_{001} = 0.099$ Å^{-1} and $q_{002} = 0.198$ Å^{-1} resulting from the lamellar periodic structure ($d = 2\pi/q_{001} = 63.47$ Å) with DNA intercalated between cationic lipid analogous to the structure in DOPC/DOTAP–DNA complexes (Fig. 2).

For $0.7 < \Phi_{PE} < 0.85$, the peaks of the SAXS scans of the CL/DNA complexes are indexed perfectly on a two-dimensional (2D) hexagonal lattice with a unit cell spacing of $a = 4\pi/[(3)^{0.5}q_{10}] = 67.4$ Å for $\Phi_{PE} = 0.7$. Figure 10 at $\Phi_{PE} = 0.7$ shows the first four order Bragg peaks of this hexagonal structure at $q_{10} = 0.107$ Å^{-1}, $q_{11} = 0.185$ Å^{-1}, $q_{20} = 0.214$ Å^{-1}, and $q_{21} = 0.283$ Å^{-1}. The structure is consistent with a 2D columnar inverted hexagonal structure (Fig. 11), which we refer to as the $H_{II}{}^C$ phase of CL/DNA complexes. The DNA molecules are surrounded by a lipid monolayer with the DNA/lipid inverted cylindrical micelles arranged on a hexagonal lattice. The structure resembles that of the inverted hexagonal H_{II} phase of pure DOPE in excess water (Seddon, 1989; Gruner, 1989), with the water space inside the lipid micelle filled by DNA. Assuming again an average lipid monolayer thickness of 20 Å, the diameter of micellar void in the $H_{II}{}^C$ phase is close to 28 Å, again sufficient for a DNA molecule with approximately two hydration shells. For $\Phi_{PE} = 0.65$ the $L_\alpha{}^C$ and $H_{II}{}^C$ structures coexist as shown in Fig. 10 (arrows point to the (001) and q_{DNA} peaks of the $L_\alpha{}^C$ phase) and are nearly epitaxially matched with $a \approx d$. For $\Phi_{PE} > 0.85$, the $H_{II}{}^C$ phase coexists with the H_{II} phase of pure DOPE, which has peaks at $q_{10} = 0.0975$ Å^{-1}, $q_{11} = 0.169$ Å^{-1}, $q_{20} = 0.195$ Å^{-1} with a unit cell spacing of $a = 74.41$ Å.

C. The Role of the Neutral Helper Lipid and Cationic Lipid in Controlling the Interaction Free Energy in DNA/Cationic Liposome Complexes: The Lamellar and Hexagonal Phases of CL/DNA Complexes

To understand the stability of the lamellar and hexagonal phases we consider the interplay between the electrostatic and membrane elastic interactions in the CL/DNA complexes that is expected to determine the different structures. Recent theoretical work suggests that electrostatic interactions alone are expected to favor the inverted hexagonal $H_{II}{}^C$ phase (Fig. 11) over the lamellar $L_\alpha{}^C$, which minimizes the charge separation between the anionic groups on the DNA chain and the cationic lipids (May and Ben-Shaul, 1997; Dan, 1998). However, the electrostatic in-

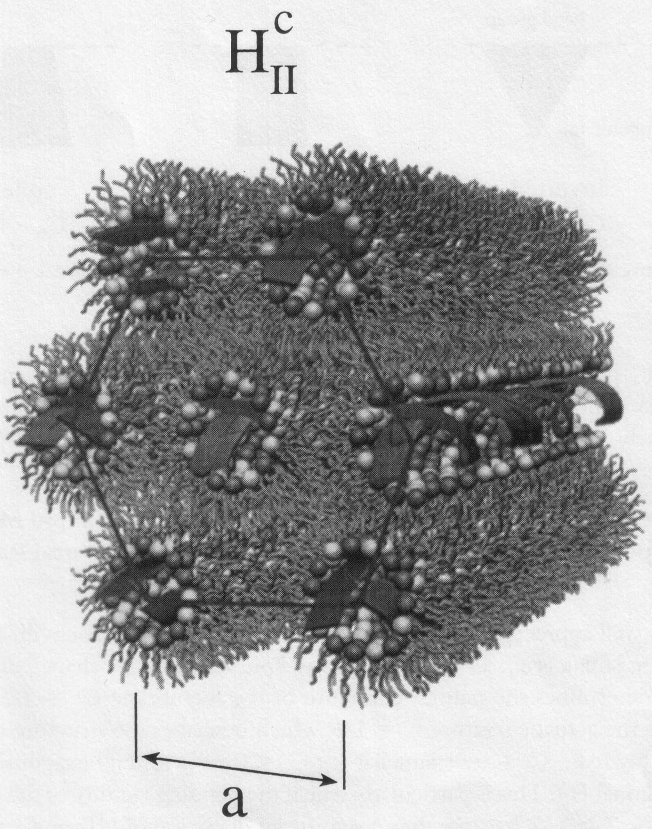

Figure 11 Schematic of the inverted hexagonal H_{II}^{C} phase (cylinders consisting of DNA coated with a lipid monolayer arranged on a hexagonal lattice) of cationic lipid/DNA (CL/DNA) complexes. [Adapted from Koltover *et al.*, (1998).]

teraction may be resisted by the membrane elastic cost (per unit area) (Seddon, 1989; Gruner, 1989; Israelachvili, 1978; Helfrich, 1978; Janiak *et al.*, 1979) of forming a cylindrical monolayer membrane around DNA:

$$F/A = 0.5\,\kappa\,(1/R - 1/R_o)^2 \qquad (1)$$

Here, κ is the lipid monolayer bending rigidity, R is the actual radius, and R_o is the natural radius of curvature of the monolayer. Figure 12 shows schematically the possible "shapes" of many common lipids. For example, many lipids (e.g., phosphatidylcholine, phosphatidylserine, phosphotidylglycerol, cardiolipin) have a cylindrical shape, with the head group area $\approx$ the hydrophobic tail area, and tend to self-assemble into lamellar structures with a natural curvature $C_o = 1/R_o = 0$. Other

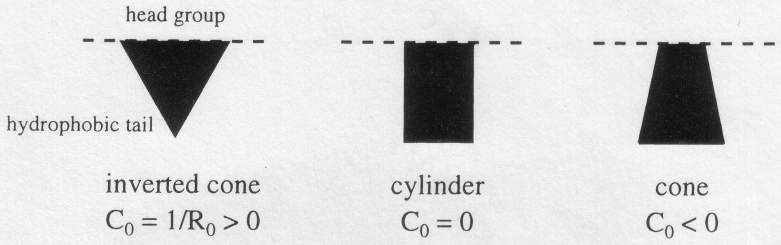

Figure 12 Three possible shapes of common lipid molecules as described in the text.

lipids (e.g., phosphotidylethanolamine) have a cone shape, with a smaller head group area than tail area, and give rise to a negative natural curvature $C_o < 0$. Alternatively, lipids with a larger head group than tail area have $C_o > 0$.

1. Control of CL/DNA Structure by Varying Shapes of Lipid Molecules: Helper Lipid and Cationic Lipid May Modify the Natural Radius of Curvature of Cationic Membranes

It is well appreciated (Seddon, 1989; Gruner, 1989; Israelachvili, 1978; Helfrich, 1978; Janiak *et al.*, 1979) that in many lipid systems the "shape" of the molecule that determines the natural curvature of the membrane $C_o = 1/R_o$ will also determine the actual curvature $C = 1/R$ which describes the structure of the lipid self-assembly (e.g., $C_o = 0 \rightarrow$ lamellar L_α; $C_o < 0 \rightarrow$ inverted hexagonal H_{II}; $C_o > 0 \rightarrow$ hexagonal H_I). This is particularly true if the bending rigidity of the membrane is large ($\kappa/k_BT >> 1$), because then a significant deviation of C from C_o would cost too much elastic energy. However, we see from Eq. (1) that if the bending cost is low with $\kappa \approx k_BT$, then C may deviate from C_o without costing much elastic energy, especially if another energy, is lowered in the process. Here we present experimental data pertaining to both situations: first, where the bending rigidity is large and the structure of the self-assembly is controlled by the "shape" of the molecule (described in the next paragraph), and second, where we lower κ enough that we find that C deviates from C_o due to the electrostatic energy favoring a different curvature and structure (described in Sect. C.2).

In the previous section we described recent synchrotron small-angle X-ray scattering (SAXS) studies in CL/DNA complexes using λ-DNA as a function of increasing Φ_{DOPE}, the weight fraction of DOPE in the DOPE/DOTAP cationic liposome mixtures (Koltover *et al.*, 1998). We found that the internal structure of the complex undergoes a structural transition from the $L_\alpha{}^C$ to the $H_{II}{}^C$. We can understand the $L_\alpha{}^C$ to $H_{II}{}^C$ transition as a function of increasing Φ_{DOPE} (Fig. 10) by noting that in contrast to the helper lipid DOPC and the cationic lipid DOTAP (Fig. 3), which have a zero natural curvature ($C_o{}^{DOTAP,DOPC} = 1/R_o{}^{DOTAP,DOPC} = 0$),

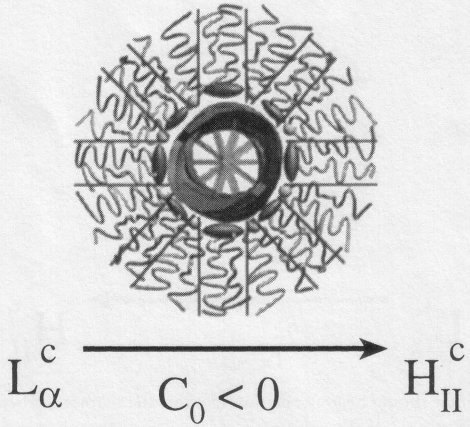

Figure 13 The H_{II}^C phase is expected to be the stable structure when the natural curvature (C_o) of the cationic lipid monolayer is driven negative by the addition of the helper lipid DOPE. This is shown schematically where the cationic lipid DOTAP is cylindrically shaped, while DOPE is cone-like with negative natural radius of curvature.

DOPE is cone shaped with $C_o^{DOPE} = 1/R_o^{DOPE} < 0$ (Fig. 12). Thus, the natural curvature of the monolayer mixture of DOTAP and DOPE is driven negative with $C_o = 1/R_o = \Phi_{DOPE}\, C_o^{DOPE}$. Hence, as a function of increasing Φ_{DOPE} we expect a transition from the L_α^C to the H_{II}^C phase (shown schematically in Fig. 13), which is observed experimentally and is now also expected to be favored by the elastic free energy. Thus, the helper lipid DOPE induces the L_α^C to H_{II}^C transition by controlling the spontaneous radius of curvature R_o of the lipid layers.

2. Control of CL/DNA Structure by Varying the Lipid Bilayer Bending Modulus through Modification of Helper Lipid: Electrostatic Energy Overwhelms the Membrane Elastic Energy as the Latter Is Reduced

The L_α^C to H_{II}^C transition was recently observed to occur along a different path by reducing the bending rigidity k of the lipid layer shown schematically in Fig. 14 (Koltover *et al.*, 1998). The reduction of κ along this pathway reduces the membrane elastic energy (determined by Eq. (1)), which otherwise prevents the formation of the H_{II}^C phase favored by electrostatics. In these experiments a new class of helper lipid molecules was used consisting of DOPC mixed with the membrane-soluble cosurfactant molecule hexanol (Koltover *et al.*, 1998). Although cosurfactant molecules, which typically consist of long-chain alcohols (e.g., pentanol, hexanol), are not able to stabilize an interface separating hydrophobic and hydrophilic regions, when mixed in with longer chain "true" surfactants they are

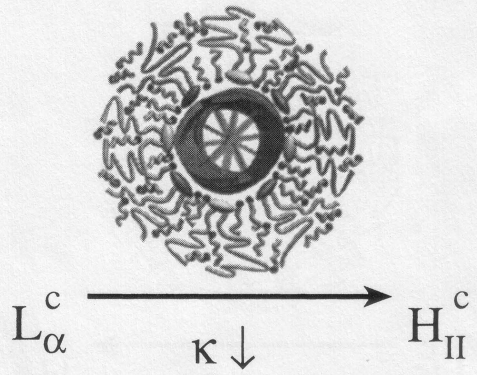

Figure 14 The H_{II}^C phase should be generally found when the membrane bending rigidity is lowered by thinning the membrane. One mechanism is to add cosurfactant molecules with short hydrophobic chains to the helper lipid as described.

known to lead to dramatic changes in interface elasticities. Simple compressional models of surfactant chains show that the bending rigidity of membranes κ scales with chain length l_n ($\propto \delta_m$, membrane thickness, n = number of carbons per chain) and the area per lipid chain A_L as $\kappa \propto l_n^3 / A_L^5$ (Szleifer *et al.*, 1988, 1990). The mixing of cosurfactants with lipids is expected to lead both to a thinner membrane and to a larger area per chain (Fig. 14) and result in a strong suppression of κ making the membrane highly flexible. Experimental studies have shown that the addition of cosurfactants like pentanol, hexanol, and heptanol to membranes of lamellar phases with a mole ratio of between two to four leads to a significant decrease of κ from about 20 $\kappa_B T$ to about 2–5 $k_B T$ (Safinya *et al.*, 1989; Safinya *et al.*, 1986).

D. The Relation between the Structure of CL/DNA Complexes and DNA Release from Complexes: Toward a Simple Model System for Studies of Transfection Efficiency

A major goal of research on CL/DNA complexes is to elucidate the key parameters resulting in the different CL/DNA complex structures and to establish the correlation between the different structures and transfection efficiency. It is known that transfection efficiency mediated by mixtures of cationic lipids and neutral helper lipids varies widely and unpredictably (Zhu *et al.*, 1993; Nabel *et al.*, 1993; Mulligan, 1993; Felgner and Rhodes, 1991; Behr, 1994; Remy *et al.*, 1994; Singhal and Huang, 1994; Lasic and Templeton, 1996). The choice of the helper lipid has been empirically established to be important (Felgner *et al.*, 1994; Farhood

et al., 1995; Hui *et al.*, 1996); for example, many papers report that transfection is believed to be significantly more efficient in mixtures of the cationic lipid DOTAP and the neutral helper lipid DOPE, then in mixtures of DOTAP and the similar helper lipid DOPC (Fig. 3). From X-ray diffraction work (Raedler *et al.*, 1997; Spector and Schnur, 1997; Seachrist, 1997; Salditt *et al.*, 1997; Safinya *et al.*, 1998; Raedler *et al.*, 1998; Salditt *et al.*, 1998) we know that DOTAP/DOPC/λ-DNA complexes form the multilamellar $L_{\alpha}{}^{C}$ structure (Fig. 2). Our work described previously shows that DOTAP/DOPE/λ-DNA containing complexes may also form the distinctly different self-assembled inverted hexagonal $H_{II}{}^{C}$ structure.

The data represent one example of a correlation between the self-assembled structure of CL/DNA complexes and transfection efficiency for this particular concentration regime in DOTAP/DOPE and DOTAP/DOPC complexes: the empirically established more transfectant DOPE-containing complexes in mammalian cell culture exhibit the $H_{II}{}^{C}$ structure rather than the $L_{\alpha}{}^{C}$ found in DOPC-containing complexes. What makes the $H_{II}{}^{C}$ structure more transfectant than the $L_{\alpha}{}^{C}$ structure? Studies show that if complexes are physically microinjected into the nucleus, expression of reporter gene is strongly suppressed; thus, under normal entry circumstances plasmid DNA must be released from the complex in the cytoplasm before translocating into the nucleus (Zabner *et al.*, 1995). In particular, since DNA has to be released from the complex before expression can occur, it is clear that mechanisms of DNA release inside cells affect (and in most instances) increase transfection efficiency (Legendre and Szoha, 1992). As described next optical microscopy studies of interactions between CL/DNA complexes and giant anionic vesicles (i.e., models of cellular membranes, in particular, anionic endosomes and plasma membranes) have directly revealed such destabilizing events (Koltover *et al.*, 1998).

1. The Stability of CL/DNA Complexes: Fusion of Cationic Liposome–DNA Complexes with Oppositely Charged Giant Vesicles (Models of Cellular Membranes)

The importance of the precise self-assembled structures to biological function is underscored in optical imaging experiments described in this section, which show that interactions of CL/DNA complexes with anionic giant liposomes (model cell membranes) are structure dependent (e.g., $H_{II}{}^{C}$ versus $L_{\alpha}{}^{C}$). One of the simpler experimental designs that we have used to look for the effect of structure on the early stages of transfection (i.e., DNA release within cells) includes light microscopy studies of the interaction of CL/DNA complexes with giant anionic vesicles that are models of CL/DNA complexes interacting with cellular membranes and anionic endosomal vesicles (Koltover *et al.*, 1998). Current data from several laboratories (Zabner *et al.*, 1995; Wrobel and Collins, 1995; Legendre and Szolca, 1992; Lin *et al.*, in preparation) indicate that one of the main entry routes of complexes is endocytosis following attachment of the positive CL/DNA complexes to negatively

charged cell surface proteoglycans (Mislich and Baldeschwieler, 1996). Thus, in many instances at the very early stages of cell transfection, an intact CL/DNA complex is captured inside an endosome that contains anionic lipids.

We have found that positively charged $H_{II}{}^{C}$ and $L_{\alpha}{}^{C}$ complexes containing DOTAP interact very differently with giant vesicles (G-vesicles) even when both types of structures contained DOPE. Figure 15 (A and B) shows video-enhanced optical microscopy in differential-interference-contrast (DIC) and fluorescence configurations, for $H_{II}{}^{C}$ (A, $\Phi_{DOPE} = 0.73$) and $L_{\alpha}{}^{C}$ (B, $\Phi_{DOPE} = 0.3$) complexes. Typical micrographs of positively charged (DOTAP/DNA = 4) complexes attached to the fluid membranes of G-vesicles show that the $L_{\alpha}{}^{C}$ complexes attach to the G-vesicles and remain stable (Fig. 15C); no fusion occurs between the complex and

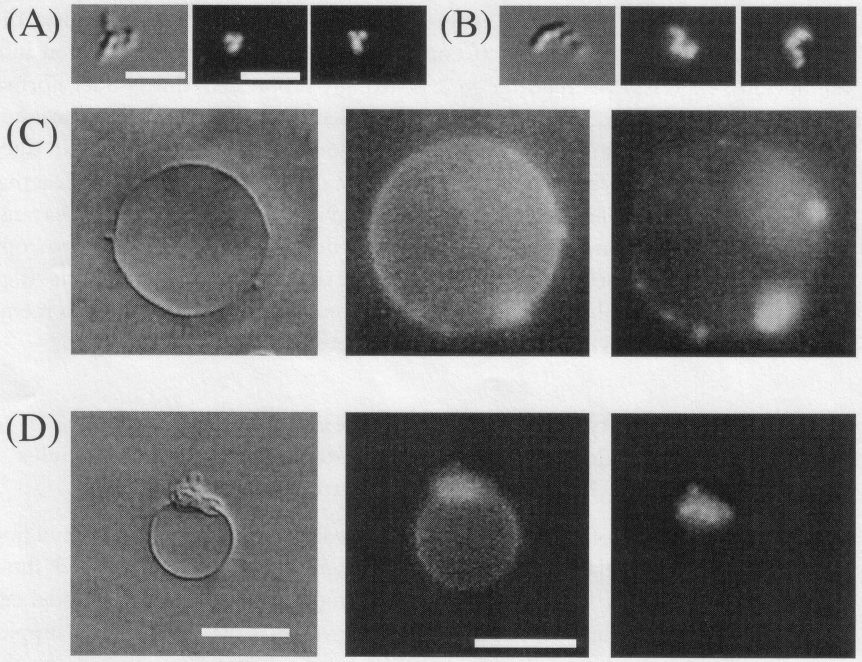

Figure 15 Video-microscopy images of positively charged CL/DNA complexes in the (A) $H_{II}{}^{C}$ and (B) $L_{\alpha}{}^{C}$ phases, and interacting with negatively charged giant (G) vesicles (C and D). In all cases, complexes were viewed in (DIC) (left), lipid fluorescence (middle), and DNA fluorescence (right). The scale bar for DIC is 3 μm for (A) and (B) and 20 μm for (C) and (D), in fluorescence image is 6 μm for (A) and (B) and 20 μm for (C) and (D). In (C) the $L_{\alpha}{}^{C}$ complexes simply stick to the G-vesicle and remain stable for many hours, retaining their blob-like morphology. The blobs are localized in DIC as well as lipid and DNA fluorescence modes. In (D), the $H_{II}{}^{C}$ complexes break up and spread immediately after attaching to G-vesicles, indicating a fusion process between the complex and the vesicle lipid bilayer and release of DNA. The loss of the compact structure of the complex is evident in both lipid and DNA fluorescence modes. [Adapted from Koltover *et al.*, (1998).]

the G-vesicle. L_α^C complexes containing DOPC show the same behavior. When H_{II}^C complexes attach to the G-vesicle, they rapidly fuse and lose their compact structure (Fig. 15D, left). The loss of the compact complex structure and the subsequent desorption of DNA molecules from membrane are seen in fluorescence (Fig. 15D right). This behavior is expected after fusion, which results in the mixing of cationic lipid (from the H_{II}^C complex) with anionic lipid (from the G-vesicle), effectively "turning off" the electrostatic interactions (which gave rise to the compact CL/DNA complexes) and releasing of DNA molecules inside the space between the lamellae and the G-vesicle bilayer. Because the geometry is the inverse of CL/DNA complexes inside anionic endosomal vesicles, we expect that upon fusion the inverse geometry will occur with DNA released and expelled outside the endosome within the cytoplasm. On longer time scales (a few hours) we observed lipid transfer between the L_α^C complexes and G-vesicles. Thus, the observation that DOPE/DOTAP L_α^C and DOPC/DOTAP L_α^C complexes do not fuse with G-vesicles is a kinetic rather than equilibrium effect. One may, in principle, be able to design L_α^C complexes with a lower kinetic barrier to fusion. Moreover, the behavior described in this review of complexes containing univalent cationic lipids may be different from that of multivalent cationic lipids. The data give evidence that H_{II}^C complexes may fuse with endosomal vesicles in cells and thus release their DNA cargo into the cytoplasm, resulting in higher transfection levels. Fluorescence microscopy studies in mouse fibroblast cell cultures, while showing more complex behavior overall, also show some similar features (Lin *et al.*, in preparation).

The findings described in Section II unambiguously establish one particular correlation between the self-assembled structure of CL/DNA complexes and transfection efficiency: for a range of concentrations the empirically established transfectant complexes in mammalian cell cultures exhibit the H_{II}^C structure rather than the L_α^C. We caution that we believe that highly transfectant L_α^C complexes may be designed in certain concentration regimes (Lin *et al.*, in preparation). Further, optical microscopy reveals a most likely origin for why different structures transfect cells with varying efficiency: in contrast to L_α^C complexes, H_{II}^C complexes are found to fuse and release DNA when in contact with anionic vesicles, which are cell free models of cellular organelle membranes, in particular, anionic endosomal vesicles. Thus, the data suggest a simple direct mechanism of DNA release into the cytoplasm from endosomal vesicles containing H_{II}^C complexes. This then paves the way for a fundamental understanding of the early-stage events following the endocytic uptake of CL/DNA complexes by mammalian cells in nonviral gene delivery applications.

III. FUTURE DIRECTIONS

Clearly much work remains before we have a complete understanding of the various possible self-assembled structures in CL/DNA complexes and an understanding, at the molecular and self-assembled levels, of all of the critical parameters

that control the different structures. Even more work will be required to relate the structures to biological function, namely, the interactions of CL/DNA complexes with cellular components inside animal cells that lead to gene release and expression. The broad, long-term objective of our research is to develop a fundamental science base that will lead to the design and synthesis of optimal nonviral carriers of DNA for gene therapy and disease control. Simultaneously, a major long-term objective is to improve efficiency for delivering large pieces of DNA containing important human genes and their regulatory sequences (> 100k base pairs), which at present can only be achieved with synthetic vectors. The structure–function data obtained from the research should allow us to begin the formidable task of a rational design of these self-assemblies for enhanced gene delivery applications from the ground up beginning with the chemical structure of the lipids and the correct compositions in mixtures including functional plasmid.

ACKNOWLEDGMENTS

First, we greatfully acknowledge the contributions of our collaborators Joachim Raedler, Tim Salditt, Alison Lin, Nelle Slack, Ayesha Ahmad, Cyril George, Charles Samuel, Uwe Schulze, and Hans-Werner Schmidt. It is a pleasure to acknowledge discussions with R. Bruinsma, A. Ben-Shaul, P. Pincus, W. Gelbart, T. Lubensky, and N. Dan. We would also like to acknowledge numerous enlightening discussions with Philip Felgner. Supported by the UC-Biotechnology Research and Education Program Grant No. 97–02, by NSF-DMR-9624091, PRF-31352-AC7, and Los Alamos-STB/UC:96–108. Partially supported by NIH-GM59288-01. The Materials Research Laboratory at Santa Barbara is supported by NSF-DMR-9632716. The X-ray experiments were carried out at the Stanford Synchrotron Radiation Laboratory supported by the U.S. Department of Energy.

REFERENCES

Behr, J. P. (1994). Gene transfers with synthetic cationic amphiphiles—prospects for gene therapy, *Bioconjugate Chem.* **5,** 382–389.

Bloomfield, V. A. (1991). Condensation of DNA by multivalent cations—considerations on mechanism, *Biopolymers* **31,** 1471–1481.

Brigham, K. L., Meyrick, B., Christman, B., Magnuson, M., King, G., and Berry, L. C. (1989). *In vivo* transfection of murine lungs with a functioning prokaryotic gene using a liposome vehicle, *Am. J. Med. Sci.* **298,** 278–281.

Bruinsma, R. (1998). Electrostatics of DNA cationic lipid complexes: isoelectric instability, *Eur. Phys. J. B* **4,** 75–88.

Bruinsma, R., and Mashl, J. (1998). Long-range electrostatic interaction in DNA cationic lipid complexes, *Europhys. Lett.,* **41,** (2), 165–170.

Crystal, R. G. (1995). Transfer of genes to humans—early lessons and obstacles to success", *Science* **270,** 404–410.

Dan, N. (1998). The structure of DNA complexes with cationic liposomes—cylindrical or flat bilayers?, *Biochim. Biophys. Acta* **1369,** 34–38.

Farhood, H., Serbina, N., and Huang, L. (1995). The role of dioleoyl phospatidylethanolamine in cationic liposome mediated gene therapy, *Biochim. Biophys. Acta* **1235,** 289–295.

Felgner, P. L. (1997). Nonviral strategies for gene therapy, *Sci. Am.* **276,** 102–106.

Felgner, P. L., Gadek, T. R., Holm, M., Roman, R., Chan, H.W., Wenz, M., Northrop, J. P., Ringold, G. M., and Danielsen, M. (1987). Lipofection: A highly efficient, lipid-mediated DNA-transfection procedure, *Proc. Nat. Acad. Sci. USA* **84,** 7413–7417.

Felgner, P. L., Rhodes, G. (1991). Gene therapeutics, *Nature* **349,** 351–352.

Felgner, J., *et al.,* (1994). Enhanced gene delivery and mechanism studies with a novel series of cationic lipid formulations, *J. Biol. Chem.* **269,** 2550–2561.

Friedmann, T. (1997). Overcoming obstacles to gene therapy, *Sci. Am.* **276,** 96–101.

Golubovic, L., and Golubovic, M. (1998). Fluctuations of quasi-two-dimensional smectics intercalated between membranes in multilamellar phases of DNA cationic lipid complexes, *Phys. Rev. Lett.* **80,** 4341–4344.

Gruner, S. M. (1989). Stability of lyotropic phases with curved interfaces, *J. Phys. Chem.* **93,** 7562–7570.

Gustafsson, J., Arvidson, G., Karlsson, G., and Almgren, M. (1995), Complexes between cationic liposomes and DNA visualized by cryo-TEM, *Biochim. Biophys. Acta* **1235,** 305–312.

Harries, D., May, S., Gelbart, W. M., and Ben-Shaul, A. (1998). Structure, stability, and thermodynamics of lamellar DNA-lipid complexes, *Biophys. J.* **75,** 159–173.

Harrington, J. J., Van Bokkelen, G., Mays, R. W., Gustashaw, K., and Williard, H. F. (1997). Formation of de novo centromeres and construction of first-generation human artificial microchromosomes, *Nature Gene.* **15,** 345–355.

Hazinski, T. A., Ladd, P. A., and Dematteo, C. A. (1991). Localization and induced expression of fusion genes in the rat lung, *Am. J. Respir. Cell Mol. Biol.* **4,** 206–209.

Helfrich, W. (1978). Steric interaction of fluid membranes in multilayer systems, *Zeitschift fur Naturforschung A* **33,** 305–315.

Holt, C. E., Garlick, N., and Cornel, E. (1990). Lipofection of CDNAS in the embryonic vertebrate central nervous system, *Neuron* **4,** 203–214.

Hui, S. W., Langner, M., Zhao, Y. L., Ross, P., *et al.* (1996). The role of helper lipids in cationic liposome-mediated gene transfer, *Biophys. J.* **71,** 590–599.

Israelachvili, J. N. (1992). *Intermolecular and surface forces* (2nd Ed.) London: Academic Press.

Janiak, M. J., Small, D. M., and Shipley, G. G. (1979). Temperature and compositional dependence of the structure of hydrated dimyristoyl lecithin, *J. Biol. Chem.* **254,** 6068–6078.

Koltover, I., Salditt, T., Raedler, J. O., and Safinya, C. R. (1998). An inverted hexagonal phase of DNA-cationic liposome complexes related to DNA release and delivery, *Science* **281,** 78–81.

Lasic, D., and Templeton, N.S. (1996). Liposomes in gene therapy, *Adv. Drug Del. Rev.* **20,** 221–266.

Lasic, D. D., Strey, H. H., Stuart, M. C. A., Podgornik, R., and Frederik, P. M. (1997). The structure of DNA-liposome complexes, *J. Am. Chem. Soc.* **119,** 832–833

Legendre, Y. J., and Szoka, F. C. (1992). Delivery of plasmid DNA into mammalian cell lines using PH-sensitive liposomes—comparison with cationic liposomes, *Pharm. Res.* **9,** 1235–1242.

Lewin, B. (1997). B: *Genes VI.* Oxford: Oxford University Press.

Lin, A., Slack, N., Ahmad, A., George, C., Samuel, C., and Safinya, C. R. Manuscript in preparation.

Livolant, F., and Leforestier, A. (1996). Condensed phases of DNA: structures and phase transitions, *Prog. Poly. Sci.* **21,** 1115–1164.

Malone, R. W. (1989). Expression of chloramphenicol acetyltransferase activity in brain tissue of frog embryos with cationic liposome vectors, *Focus* **11,** 4.

Manning, G. S. (1969). Limiting laws and counterion condensation in polyelectrolyte solutions. I. Colligative properties, *J. Chem. Phys.* **51,** 924–933.

Marshall, E. (1995). Gene therapys growing pains, *Science* **269,** 1050–1055.

May, S., and Ben-Shaul, A. (1997). DNA-lipid complexes: Stability of honeycomb-like and spaghetti-like structures, *Biophys. J.* **73,** 2427–2440.

Miller, A. D. (1998). Cationic liposomes for gene therapy, Angewandte Chemie (Intl. Ed.), *Reviews* **37,** 1768–1785.

Mislick, K. A. and Baldeschwieler, J. D. (1996). Evidence for the role of proteoglycans in cation mediated gene transfer, *Proc. Nat. Acad. Sci. USA* **93,** 12349–12354.

Mulligan, R. C. (1993). The basic science of gene therapy, *Science* **260,** 926–932.

Nabel, G. J., Nabel, E. G., Yang, Z. Y., Fox, B. A., Plautz, G. E., Gao, X., Huang. L., Shu, S., Gordon, D., and Chang, A. E. (1993). Direct gene transfer with DNA liposome complexes in melanoma-expression, biologic activity, and lack of toxicity in humans, *Proc. Nat. Acad. Sci. USA* **90,** 11307–11311.

O'Hern, C. S., and Lubensky, T. C. (1998). Sliding columnar phase of DNA lipid complexes, *Phys. Rev. Lett.* **80,** 4345–4348.

Ono, T., Fujino, Y., Tsuchiya, T., and Tsuda, M. (1990). Plasmid DNAS directly injected into mouse brain with lipofection can be incorporated and expressed by brain cells, *Neurosci. Lett.* **117,** 259–263.

Pitard, B., Aguerre, O., Airiau, M., Lachagés, A.-M., Boukhnikachvili, T., Byk, G., Dubertret, C., Herviou, C., Scherman, D., Mayaux, J.-F. and Crouzet, J. (1997). Virus sized self-assembled lamellar complexes between plasmid DNA and cationic micelles promote gene transfer, *Proc. Natl. Acad. Sci. USA 94,* 14412–14417.

Podgornik, R., Rau, D. C., and Parsegian, V. A. (1994)., Parametrization of direct and soft steric-undulatory forces between DNA double helical polyelectrolytes in solutions of several different anions and cations, *Biophys. J.* **66,** 962–971.

Raedler, J. O., Koltover, I., Salditt, T., Jamieson, A., and Safinya, C. R. (1998). Structure and interfacial aspects of self-assembled cationic lipid-DNA gene carrier complexes, *Langmuir* **14,** 4272–4283.

Raedler, J. O., Koltover, I., Salditt, T., and Safinya, C. R. (1997). Structure of DNA-cationic liposome complexes: DNA intercalation in multi-lamellar membranes in distinct interhelical packing regimes, *Science* **275,** 810–814.

Reich, Z., Wachtel, E. J., and Minsky, A. (1994). Liquid crystalline-mesophases of plasmid DNA in bacteria, *Science* **264,** 1460–1463.

Remy, J. S., Sirlin, C., Vierling, P., and Behr, J. P. (1994). Gene transfer with a series of lipophilic DNA-binding molecules, *Bioconjugate Chem.* **5,** 647–654

Roush, W. (1997). Molecular biology—counterfeit chromosomes for humans, *Science* **276,** 38–39.

Roux, D., and Safinya, C. R. (1988). A synchroton x-ray study of competing undulation and electrostatic interlayer interactions in fluid multimembrane lyotropic phases, *J. Phys. France* **49,** 307–318.

Safinya, C. R., Koltover, I., and Raedler, J. O. (1998). DNA at membrane surfaces: An experimental overview, *Cur. Opin. Colloid Interface Sci.* **3 (1),** 69.

Safinya, C. R., Sirota, E. B., Roux, D. and Smith, G. S. (1989). Universality in interacting membranes: The effect of cosurfactants on the interfacial rigidity, *Phys. Rev. Lett.* **62,** 1134.

Safinya, C. R. Rigid and fluctuating surfaces: A series of synchrotron x-ray scattering studies of interacting stacked membranes. In Riste, R., and Sherrington, D. (Eds) (1989). *Phase transitions in soft condensed matter,* NATO ASI Series B **211,** 249–270.

Safinya, C. R., Roux, D., Smith G. S., Sinha S. K., Dimon P., Clark N. A., and Bellocq A. M. (1986). Steric interactions in a model membrane system: A synchrotron x-ray study. *Phys. Rev. Lett.* **57,** 2718–2721.

Salditt, T., Koltover, I., Radler, J. O., and Safinya, C. R. (1997). Two-dimensional smectic ordering of linear DNA chains in self-assembled DNA-cationic liposome mixture, *Phys. Rev. Lett.* **79,** 2582–2585.

Salditt, T., Koltover, I., Raedler, R. O., and Safinya, C. R. (1998). Self-assembled DNA-cationic lipid complexes: Two-dimensional smectic ordering, correlations, and interactions, *Phys. Rev. E* **58,** 889–904.

Seachrist, L. (1997). Researchers weigh advantages of using liposomes to deliver DNA to cells, *Bioworld Today* (The Daily Biotechnology Newspaper) **8,** (26), February 7, p.1.

Seddon, J. M. (1989). Structure of the inverted hexagonal phase and non-lamellar phase transitions of lipids, *Biochim. Biophys. Acta* **1031,** 1–69.

Singhal, A., and Huang, L. (1994); Wolff, J. A. (Ed.), In Gene therapeutics: Methods and applications of direct gene transfer.Boston: Birkhauser.

Spector, M. S. and Schnur, J. M. (1997). DNA ordering on a lipid membrane. In *Science* (Perspectives article), **275,** 791–792.

Sternberg, B., Sorgi, F. L., and Huang, L. (1994). New structures in complex formation between DNA and cationic liposomes visualized by freeze-fracture electron microscopy, *FEBS Lett.* **356,** 361–366.

Stribling, R., Brunette, E., Liggitt, D., Gaensler, K., and Debs, R. (1992). Aerosol gene delivery *in vivo*, *Proc. Natl. Acad. Sci. (USA)* **89,** 11277–11281.

Szleifer, I., Ben-Shaul, A., and Gelbart, W. M. (1990). Chain packing statistics and thermodynamics of amphilphile monolayers, *J. Phys. Chem.* **94,** 5081–5089

Szleifer, I., Kramer, D., Ben-Shaul, A., Roux, D., and Gelbart, W. M. (1988). *Phys. Rev. Lett.* **60,** 1966.

Wrobel, I., and Collins, D. (1995). Fusion of cationic liposomes with mammalian cells occurs after endocytosis, *Biochim. Biophys, Acta* **1235,** 296–304.

Zabner, J., Fasbender, A. J., Moninger,T., Poelinger, K. A., and Welsh, M. J. (1995). Cellular and molecular barriers to gene transfer by a cationic lipid, *J. Biol. Chem.* **270,** 18997–19007.

Zhu, N., Liggitt, D., Liu, Y., and Debs, R. (1993). Systemic gene expression after intravenous DNA delivery into adult mice, *Science* **261,** 209–211.

Zimm, B. H., and Le Bret, M. (1983). Counter-ion condensation and system dimensionality, *J. Biomol. Struc. Dyn.* **1,** 461–471.

ENDNOTE

A mixture of DOPC/DOTAP (1/1, wt/wt) was prepared in a 20 mg/ml chloroform stock solution. 500 ml was dried under nitrogen in a narrow glass beaker and desiccated under vacuum for 6 h. After addition of 2.5 ml Millipore water and 2 h incubation at 40°C, the vesicle suspension was sonicated to clarity for 10 min. The resulting solution of liposomes, 25 mg/ml, was filtered through 0.2 μm Nucleopore filters. For optical measurements the concentration of SUV used was between 0.1mg/ml and 0.5 mg/ml. All lipids were purchased from Avanti Polar Lipids, Inc. (Alabaster, Alabama). For fluorescence work, sonicated DOPC-DOTAP(1/1) liposomes were prepared at 0.1mg/ml with 0.2 mol % DHPE-Texas Red fluorescence label. DNA stained by YOYO (Molecular Probes) was added under gentle mixing at different lipid to DNA ratios (L/D). For X-ray diffraction studies the DNA/lipid condensates were prepared from a 25 mg/ml liposome suspension and a 5mg/ml DNA solution. The solutions were filled in 2 mm diameter quartz capillaries with different ratios L/D respectively and mixed after flame sealing by gentle centrifugation up and down the capillary.